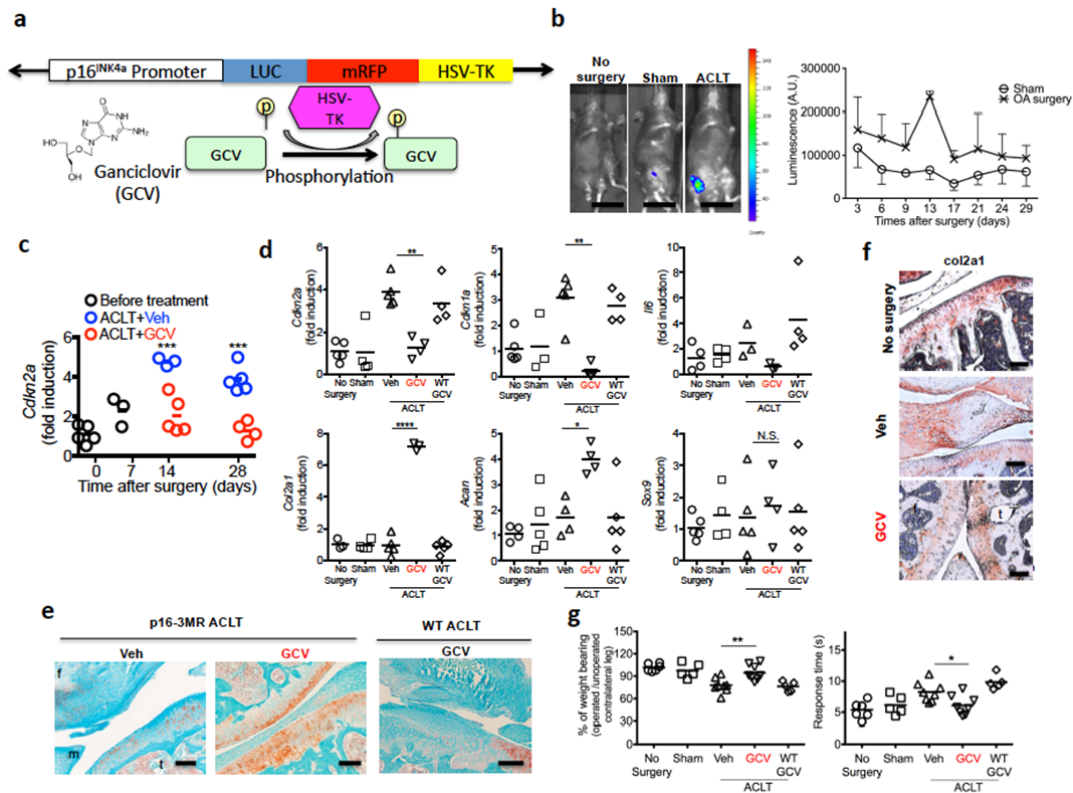


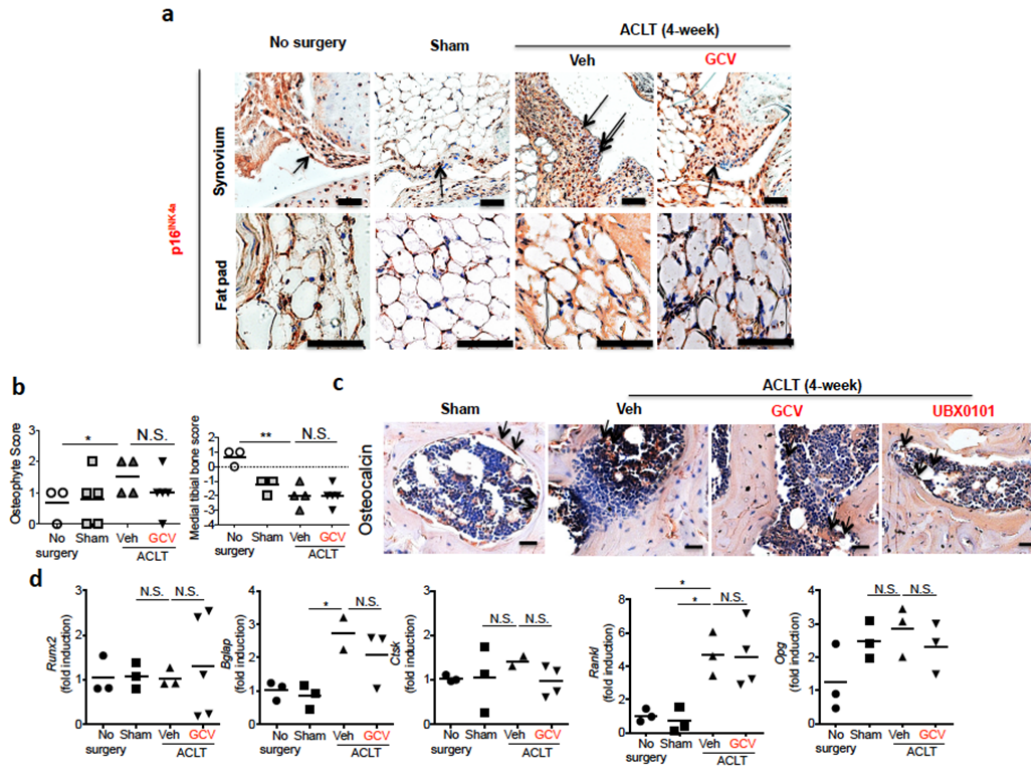
1



2

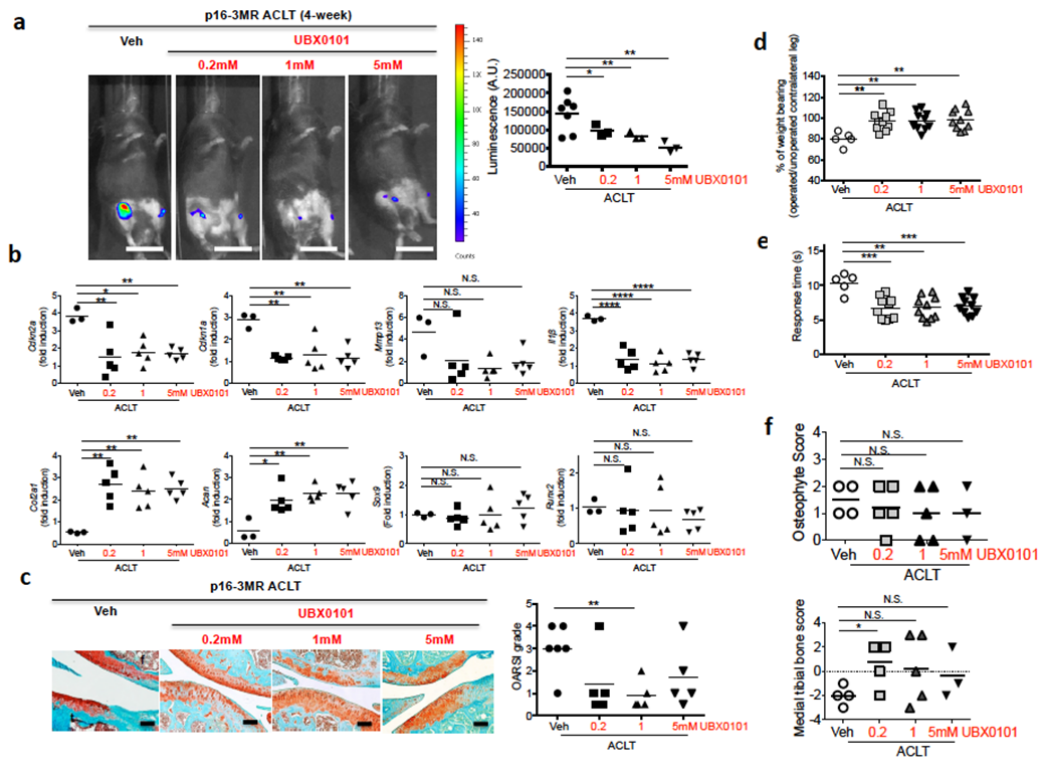
3

4 **Supplementary Figure 1. Kinetics of SnCs development in surgically-induced**  
 5 **OA and effect of GCV-induced SnC clearance on OA disease progression in**  
 6 **C57BL and p16-3MR mice.** (a) Diagram depicting the p16-3MR transgene. (b)  
 7 p16-3MR mice received vehicle (Veh, 10  $\mu$ l saline) to the ACLT-operated or sham-  
 8 operated knee by IA injection 8 days after the surgery for 5 consecutive days, with a  
 9 2<sup>nd</sup> treatment 21 days after post-surgery for 5 consecutive days. Shown are  
 10 representative images of mice 28 days post-surgery and quantification of  
 11 luminescence (in arbitrary units, A.U.) at the indicated time.  $n = 4$  for each group.  
 12 Scale bars, 2 cm. In c–g, we administered two cycles of GCV for 5 consecutive days  
 13 (1 mM in 10  $\mu$ l saline) starting at day 8 after surgery in p16-3MR or non-transgenic  
 14 C57BL mice. (c) Quantification of mRNA expression for *Cdkn2a* at indicated time  
 15 and (d) *Cdkn2a*, *Cdkn1a*, *Il6*, *Col2a1*, *Acan* and *Sox9* normalized to  $\beta$ -actin day 28  
 16 after surgery from p16-3MR mice articular joints that received Veh or GCV and non-  
 17 transgenic C57BL mice that received GCV. (e) Representative images of Safranin-  
 18 O/methyl green staining; Veh-treated p16-3MR ACLT,  $n = 1$ ; GCV-treated p16-3MR  
 19 ACLT or C57BL ACLT,  $n = 3$  and (f) *col2a1* immunohistochemistry; No surgery,  $n =$   
 20 2; Veh-treated ACLT,  $n = 6$ ; GCV-treated ACLT,  $n = 3$ , Scale bars, 100  $\mu$ m and (g)  
 21 the percentage of weight placed on the operated limb versus contralateral control limb  
 22 and response time of mice after placement onto a 55°C hotplate. \* $P < 0.05$ , \*\* $P <$   
 23 0.01, \*\*\* $P < 0.001$  and N.S. (Not Significant); one-way ANOVA (Tukey's multiple  
 24 comparison test) for c, d; unpaired t-test (two-tailed) for g. All data are expressed as  
 25 mean and each data point represents an individual mouse.



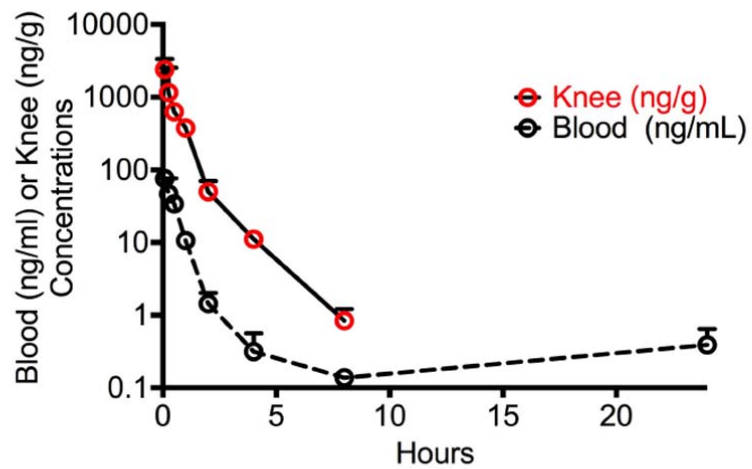
26  
27  
28  
29  
30  
31  
32  
33  
34  
35  
36  
37  
38  
39  
40  
41  
42  
43  
44  
45  
46  
47  
48  
49  
50  
51  
52  
53

**Supplementary Figure 2. The presence of SnCs in the synovium and infrapatellar fat pad, and characterization of subchondral bone changes in p16-3MR mice after vehicle or GCV-treatment.** (a) Representative images of p16<sup>INK4a</sup>-positive SnCs in the synovium and infrapatellar fat pad; No surgery and Sham-operated controls,  $n = 2$ ; Veh- or GCV treated ACLT,  $n = 3$ . Scale bars, 100  $\mu\text{m}$  (b) Scores for osteophyte formation and medial tibial bone loss. Marked osteophyte formation and subchondral bone loss were observed in veh-treated mice 28 days post-surgery, which did not significantly decrease with GCV treatment. (c) Representative images of osteocalcin. There was an increase in abnormal osteocalcin-positive osteoblasts (arrows) in the marrow area of the tibial subchondral bone are increased in abnormal in Veh, GCV and UBX0101-treated p16-3MR with ACLT surgery. In contrast, these cells were located on the bone surface of sham-operated controls. Sham-operated controls,  $n = 2$ ; Veh-treated,  $n = 4$ ; GCV-treated,  $n = 2$ ; UBX0101-treated ACLT,  $n = 5$ . Scale bars, 100  $\mu\text{m}$  (d) Quantification of mRNA expression for *Runx2* and *Bglap* (osteocalcin) as bone formation markers and *Ctsk*, *Rankl*, and *Opg* (osteoprotegerin) as bone turnover markers normalized to  $\beta$ -actin in joints. ACLT surgery resulted in an increase in expression of *Runx2* and *Bglap* and accelerated *Ctsk*, *Rankl*, and *Opg*, that did not change with GCV treatment on day 28 after surgery. In (b) and (d),  $*P < 0.05$ ,  $**P < 0.01$ , and N.S. (Not Significant); unpaired t-test (two-tailed) for b; one-way ANOVA (Tukey's multiple comparisons test) for d. All data are expressed as mean and each data point represents an individual mouse.

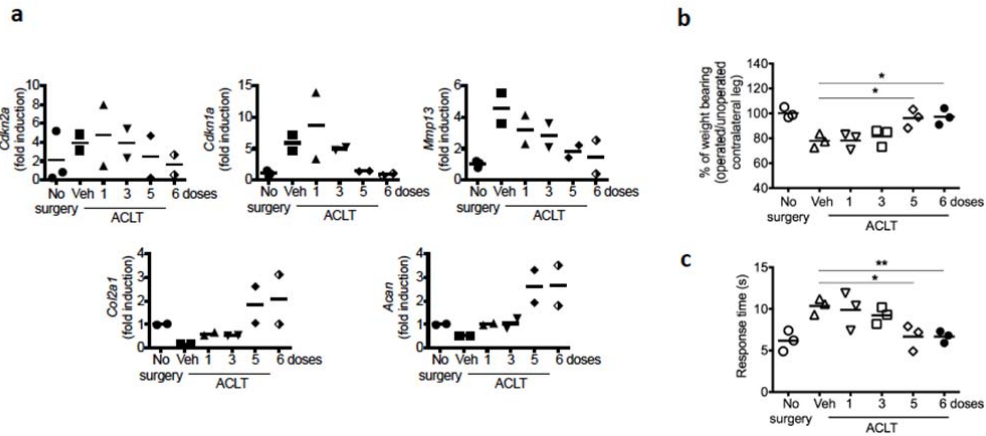


54  
 55  
 56  
 57  
 58  
 59  
 60  
 61  
 62  
 63  
 64  
 65  
 66  
 67  
 68  
 69  
 70  
 71  
 72  
 73

**Supplementary Figure 3. UBX0101 dose-dependent elimination of SnCs induced by post-traumatic OA in p16-3MR mice and resulting changes in progression of post-traumatic OA.** (a) Representative whole body luminescent images of vehicle (Veh) or 0.2, 1, and 5 mM of UBX0101-treated p16-3MR mice 28 days following IA injection once every two days over 2 weeks starting 14 days post-surgery (left). Quantification of luminescence (right). No surgery,  $n = 7$ ; 0.2, 1 or 5 mM UBX0101-treated ACLT mice,  $n = 3$ . Scale bars, 2 cm. (b) Quantification of mRNAs expression for *Cdkn2a*, *Cdkn1a*, *Mmp13*, *Il1 $\beta$* , *Col2a1*, *Acan*, *Sox9* and *Runx2* normalized to  $\beta$ -actin. (c) Representative images of Safranin-O/methyl green and comparison of Veh or 0.2, 1, and 5 mM of UBX0101-treated p16-3MR mice knee joints by OARS1 grade. No surgery,  $n = 6$ ; 0.2, 1 or 5 mM UBX0101-treated ACLT mice,  $n = 5$ . Scale bars, 100  $\mu$ m. (d) Weight bearing test and (e) hotplate analysis upon UBX0101 treatment. (f) Scores for osteophyte formation and local medial tibial bone density on day 28 after surgery. \* $P < 0.05$ , \*\* $P < 0.01$ , \*\*\* $P < 0.001$ , \*\*\*\* $P < 0.0001$  and N.S. (Not Significant); one-way ANOVA (Tukey's multiple comparisons test) for b; unpaired t-test (two-tailed) for a and c-f. All data are expressed as mean and each data point represents an individual mouse.

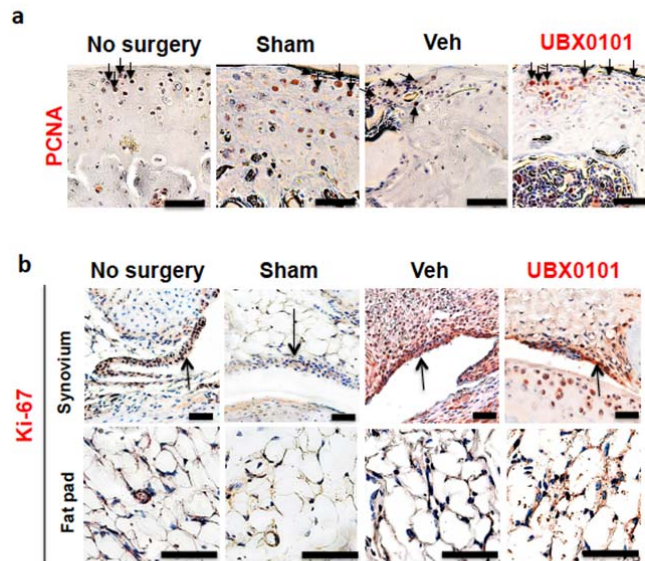


74  
 75 **Supplementary Figure 4. Local and blood pharmacokinetics (PK) of UBX0101**  
 76 **after IA injection.** C57BL mice were injected IA with 1 mM UBX0101 (in 10  $\mu$ l of  
 77 saline per knee,  $n = 2$  mice per time point). The initial dose of UBX0101 falls below  
 78 the IC<sub>50</sub> 1.5 hours following IA injection. Approximately 1/30<sup>th</sup> of the initial dose  
 79 reaches the circulation and the IC<sub>50</sub> is never reached in the circulation.  
 80

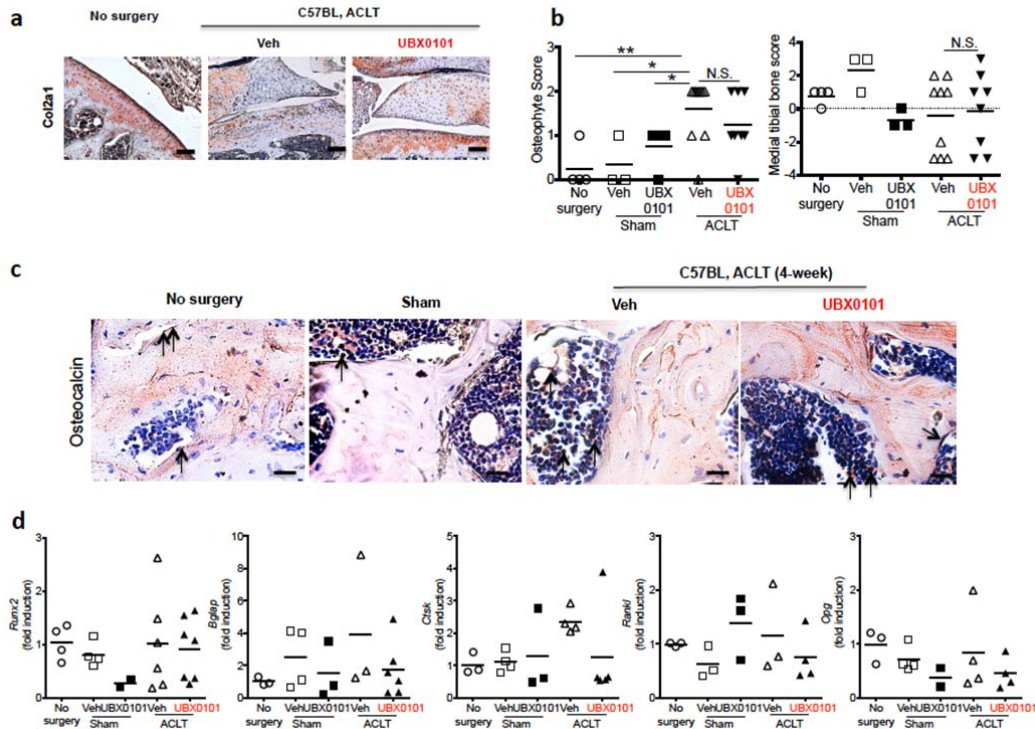


81  
 82 **Supplementary Figure 5. Efficacy of increasing UBX0101 injections on OA**  
 83 **progression.** C57BL mice that underwent the ACLT in one rear limb to induce OA  
 84 were treated every other day with vehicle (Veh) or different numbers of UBX0101 IA  
 85 injections (1 mM in 10  $\mu$ l saline, 1 to 6 injections) for 2 weeks starting 14 days post-  
 86 surgery. (a) Quantification of mRNA expression for *Cdkn2a*, *Cdkn1a*, *Mmp13*, *Il1 $\beta$* ,  
 87 *Col2a1* and *Acan* normalized to  $\beta$ -actin in joints 28 days after ACLT;  $n = 2$  for each  
 88 group. No statistical analysis. (b) The percentage of weight placed on the operated  
 89 limb versus the contralateral control limb and (c) response time after placement on a  
 90 55°C platform on day 28 after ACLT surgery. \* $P < 0.05$  and \*\* $P < 0.01$ ; two-tailed  $t$   
 91 tests (unpaired). All data are expressed as mean and each data point represents an  
 92 individual mouse.  
 93



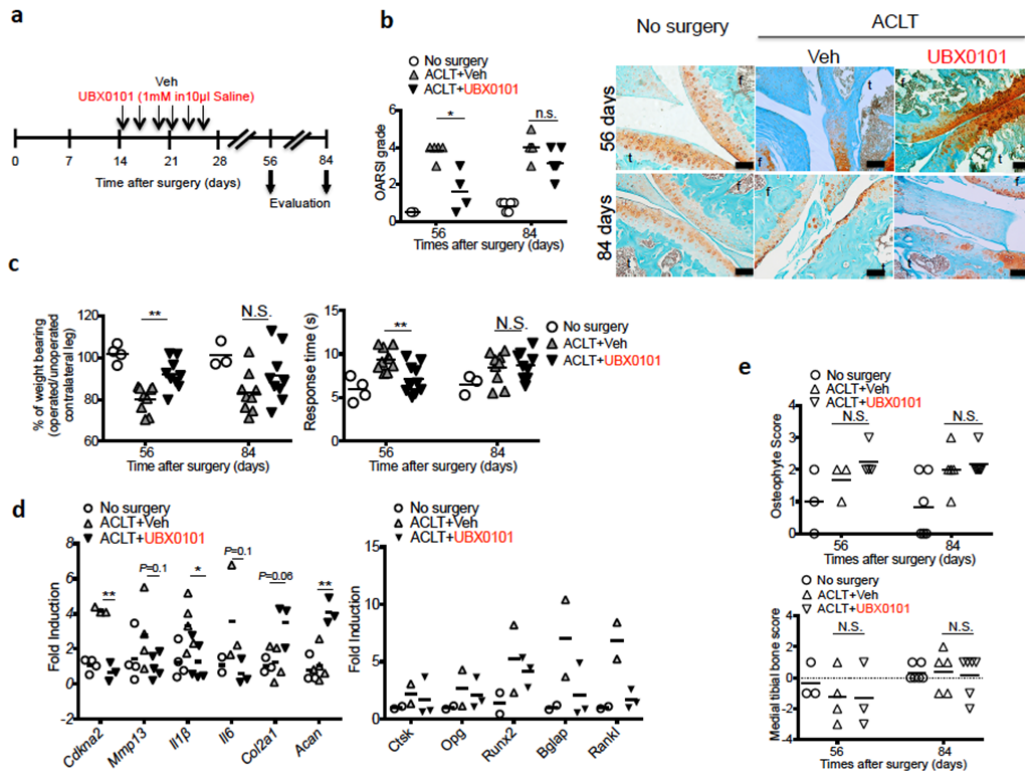


94  
 95 **Supplementary Figure 6. The PCNA-positive non-SnCs in cartilage and Ki67**  
 96 **positive non-SnCs in synovium and infrapatellar fat pad after vehicle or**  
 97 **UBX0101-treated C57BL mice. (a)** Representative images of PCNA expression by  
 98 immunohistochemistry (brown staining at arrows). There were fewer PCNA-  
 99 expressing non-SnCs in the articular cartilage of vehicle (Veh)-treated C57BL mice,  
 100 whereas increased number of PCNA positive proliferating cells in those of UBX0101-  
 101 treated mice 4 weeks after ACLT.  $n = 3$  for each group. Scale bars, 100  $\mu\text{m}$ . (b)  
 102 Representative images of Ki-67 expression (brown staining at arrows). In Veh-treated  
 103 C57BL mice, fewer Ki-67-expressing cells (hyperplastic synovial membrane, brown  
 104 staining at arrows) were detected in the synovium, consistent with the presence of  
 105 SnCs, which was abrogated by UBX0101 treatment.  $n = 3$  for each group. Scale bars,  
 106 100  $\mu\text{m}$ .  
 107



108  
 109  
 110  
 111  
 112  
 113  
 114  
 115  
 116  
 117  
 118  
 119  
 120  
 121  
 122  
 123  
 124

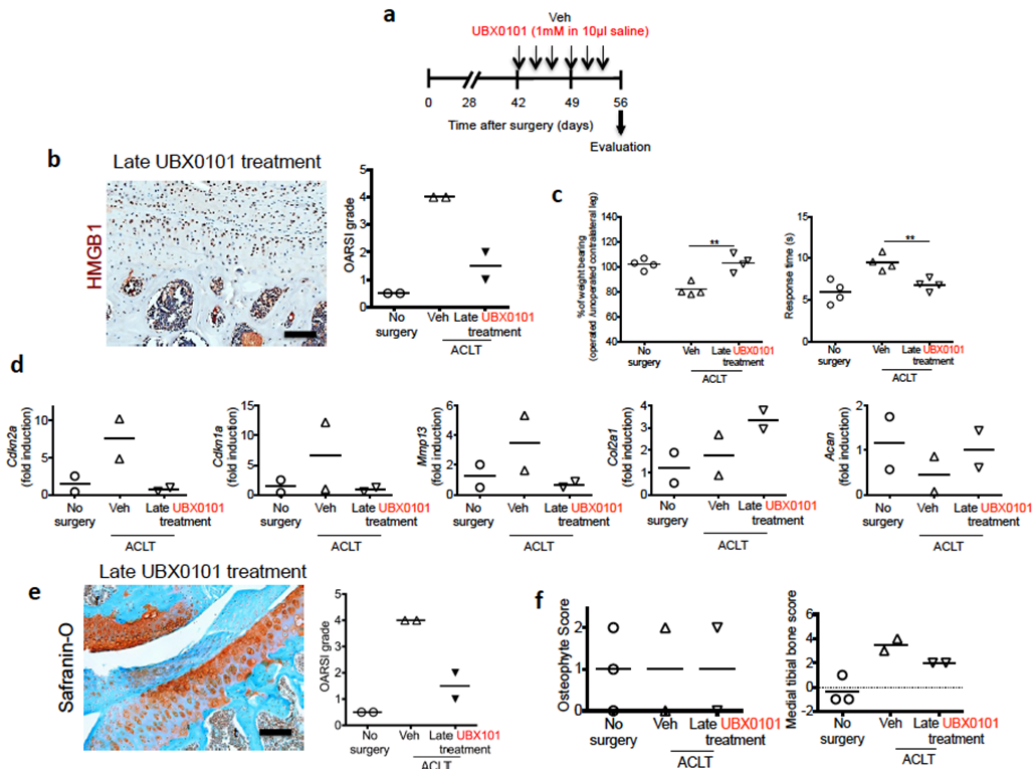
**Supplementary Figure 7. UBX0101 treatment increased type II collagen protein but did not significantly reduce subchondral bone changes in ACLT C57BL mice 28 days after the injury.** (a) Immunohistochemical analyses showed that in UBX0101-treated C57BL mice, increased type II collagen protein was detected relative to vehicle (Veh)-treated ACLT mice. No surgery,  $n = 4$ ; Veh-treated ACLT,  $n = 6$ ; UBX0101-treated ACLT,  $n = 4$ . Scale bars, 100  $\mu\text{m}$  (b) UBX0101 treatment did not significantly suppress osteophyte formation and the extent of subchondral bone loss in ACLT mice. (c) Osteocalcin-positive cells (brown staining at arrows) in tibial subchondral bone marrow collected 28 days after ACLT surgery and treatment with Veh or UBX0101. No surgery, Sham-operated and Veh-treated ACLT,  $n = 2$ ; UBX0101-treated ACLT,  $n = 3$ . Scale bars, 100  $\mu\text{m}$  (d) Quantification of the levels of mRNAs encoding *Runx2*, *Bglap*, *Ctsk*, *Rankl* and *Opg* (which encode runt related transcription factor 2, osteocalcin, cathepsin K, Receptor activator of nuclear factor kappa-B ligand and osteoprotegerin, individually) normalized to  $\beta$ -actin in joints from C57BL mice that received Veh or UBX0101 on day 28 after surgery.



125  
 126 **Supplementary Figure 8. Long-term efficacy of UBX0101 in attenuating post-**  
 127 **traumatic OA development.** (a) Schematic of time course for experiments in **b e**.  
 128 C57BL mice that underwent the ACLT of one rear limb were treated with vehicle  
 129 (Veh) or UBX0101 (1 mM in 10 µl saline) once every two days over 2 weeks starting  
 130 14 days post-surgery. (b) Left: Comparison of vehicle-treated and UBX0101-treated  
 131 knee joints 56 or 84 days after surgery by OARSIS grade. Right: Representative  
 132 images of Safranin-O/methyl green staining of the medial compartment as indicated  
 133 time. No surgery,  $n = 3$ ; Veh-treated,  $n = 5$ ; UBX0101-treated,  $n = 4$  for 56 days time  
 134 point. No surgery and UBX0101-treated,  $n = 6$ ; Veh-treated,  $n = 5$  for 84 days time  
 135 point. Scale bars, 100 µm. (c) Percentage of weight placed on the operated limb  
 136 versus contralateral control limb (left) and response time after placement onto a 55° C  
 137 platform (right). (d) Quantification of mRNA expression for *Cdkn2a*, *Mmp13*, *Il1β*,  
 138 *Il6*, *Col2a1*, *Acan*, *Ctsk*, *Opg*, *Runx2*, *Bglap* and *Rankl* normalized to  $\beta$ -actin in joints  
 139 56 days after ACLT. (e) Histological analysis of subchondral bone changes as  
 140 confirmed by osteophyte formation and bone sclerosis score. All data are expressed as  
 141 mean and each data point represents an individual mouse. \* $P < 0.05$ , \*\* $P < 0.01$ , and  
 142 N.S. (Not Significant); one-way ANOVA (Tukey's multiple comparison test) for **d**;  
 143 two-tailed t tests (unpaired) for **b**, **c**, and **e**.

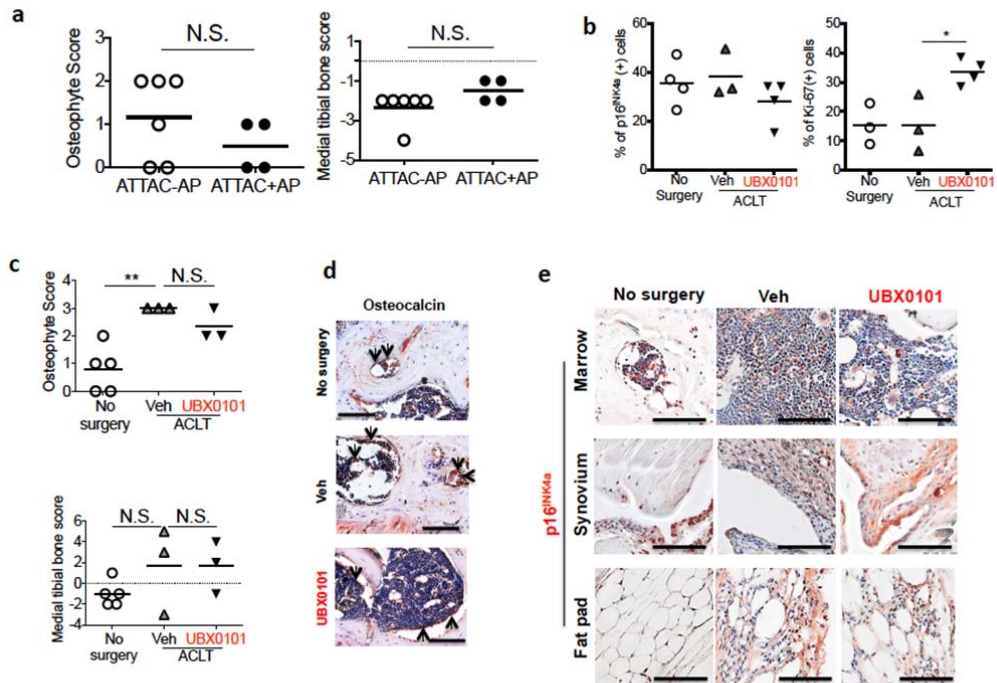
144  
 145  
 146



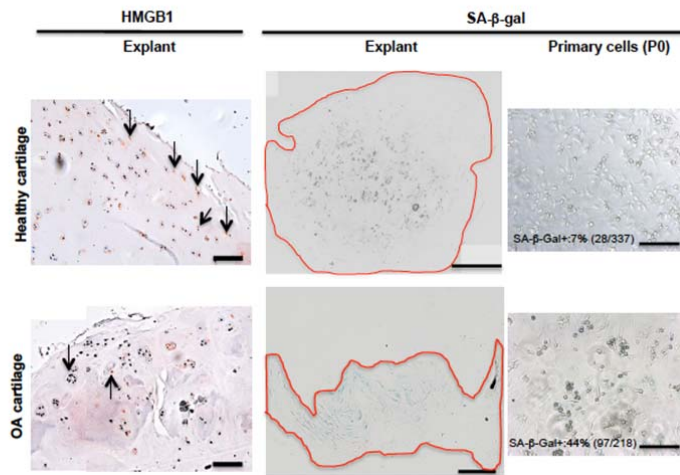


147  
148  
149  
150  
151  
152  
153  
154  
155  
156  
157  
158  
159  
160  
161  
162  
163  
164  
165  
166

**Supplementary Figure 9. Efficacy of UBX0101 for treating advanced post-traumatic OA.** (a) Schematic of experiment for b–e. C57BL mice underwent ACLT of one rear limb to induce OA and were injected IA once every two days with vehicle (Veh) or UBX0101 (1 mM in 10 µl saline) during 6 and 7 weeks post-surgery for 2 weeks. (b) Representative images of cells positive for nuclear HMGB1 by immunohistochemistry (left) and quantification of HMGB1-positive non-SnCs in articular cartilage (right).  $n = 2$ . Scale bar, 100 µm. (c) OA-induced joint pain was alleviated by UBX0101 as monitored by weight bearing and hot plate analyses on day 56 after ACLT surgery;  $n = 4$  for each group. (d) Quantification of mRNAs expression *Cdkn2a*, *Cdkn1a*, *Mmp13*, *Il1β*, *Col2a1* and *Acan* normalized to  $\beta$ -actin in joints as indicated;  $n = 2$  for each group. (e) Representative images of Safranin-O/methyl green staining of late UBX0101 treated joint (left,  $n = 2$ ) and OARS1 scores. Scale bar, 100 µm. (f) Histological analysis of parameters of subchondral bone changes at 56 days post ACLT surgery: osteophyte formation and medial tibial bone score as indicated for trabecular bone sclerosis. All data are expressed as mean and each data point represents an individual mouse. No statistical analysis.

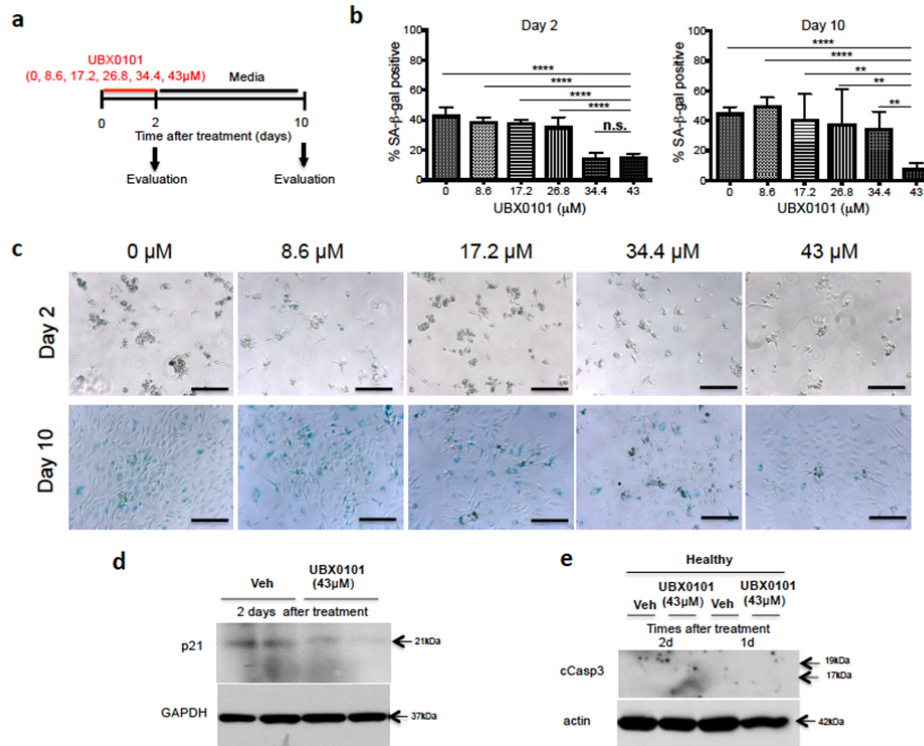


167  
 168 **Supplementary Figure 10. Characterization of bone and other joint tissue**  
 169 **changes after SnC clearance in naturally-occurring or surgically-induced INK-**  
 170 **ATTAC or p16-3MR aged mice.** (a) Subchondral bone damage scores for  
 171 osteophyte formation and medial tibial bone sclerosis in INK-ATTAC female mice  
 172 that received vehicle (-AP,  $n = 6$ ) or AP (+AP,  $n = 4$ ) according to the scheme shown  
 173 in Figure 3a. (b) Quantification of p16<sup>INK4a</sup>-positive SnCs and Ki-67-positive non-  
 174 SnCs staining in articular cartilage. (c) Subchondral bone damage scores for  
 175 osteophyte formation and medial tibial bone sclerosis and (d) osteocalcin-positive  
 176 cells in subchondral bone marrows (brown staining at arrows) by  
 177 immunohistochemistry of 19- to 20-month-old p16-3MR male mice with ACLT  
 178 surgery treated with vehicle (Veh) or UBX0101 (1 mM in 10  $\mu$ l saline, once every 2  
 179 days over 2 weeks starting 14 days post-surgery).  $n = 2$  for each group. All data are  
 180 expressed as mean and each data point represents an individual mouse. Scale bars,  
 181 100  $\mu$ m. (e) The presence of p16<sup>INK4a</sup>-positive cells in the subchondral bone marrow,  
 182 synovium and fat pad (brown) of p16-3MR mice shown by immunostaining and their  
 183 changes after UBX0101 treatment.  $n = 3$  for each group. Scale bars, 100  $\mu$ m. \* $P <$   
 184 0.05, \*\* $P <$  0.01 and N.S. (Not Significant); two-tailed t tests (unpaired).  
 185  
 186  
 187  
 188  
 189  
 190



191  
 192 **Supplementary Figure 11. Presence of SnCs in human healthy and**  
 193 **osteoarthritic articular cartilage.** Representative images of HMGB1-positive non-  
 194 SnCs (brown staining at arrows, Scale bars, 100  $\mu$ m) by immunohistochemistry and  
 195 SA- $\beta$ -gal-positive SnCs expression on the articular cartilage explant. SA- $\beta$ -gal-  
 196 positive SnCs were observed throughout the depth of osteoarthritic cartilage (donor:  
 197 65-years-old, Male), but were sparsely present in healthy cartilage (donor:  
 198 62-years-old, Male). Scale bars, 500  $\mu$ m. A range of 7-15% SA- $\beta$ -gal-positive SnCs were  
 199 observed in primary chondrocytes isolated from healthy cartilage and 41–50% SA- $\beta$ -  
 200 gal-positive SnCs were detected in the chondrocytes from osteoarthritic cartilage  
 201 (passage 0). Scale bars, 100  $\mu$ m.

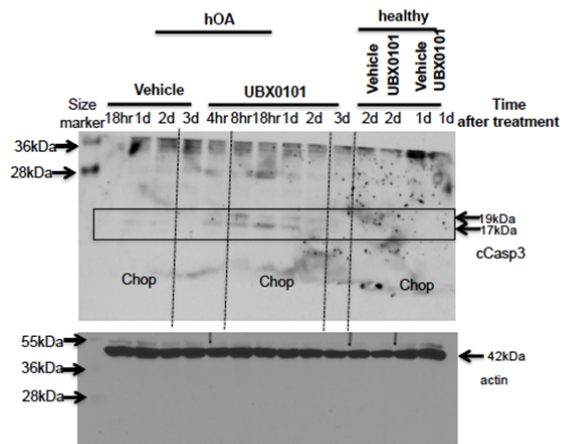
202  
 203  
 204



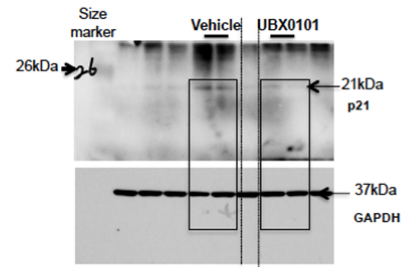
205  
206  
207  
208  
209  
210  
211  
212  
213  
214  
215  
216  
217  
218  
219  
220

**Supplementary Figure 12. Dose-dependent elimination of senescent chondrocytes isolated from human OA tissue by UBX0101 treatment.** (a) Schematic of experiment for b–c. (b) SA-β-gal positive cells were quantified 2 and 8 days following treatment with increasing concentrations of UBX0101. A dose of 43 μM and a short treatment time (2 days) selectively eliminated SA-β-gal positive senescent chondrocytes. Data are averages ± S.D. \*\**P* < 0.01, \*\*\*\**P* < 0.0001 and n.s. (Not Significant); One-way ANOVA (Tukey’s multiple comparison test). *n* = 5 for 0, 8.6 and 12.2 μM; *n* = 6 for 34.4 and 43 μM. (c) Representative images of cells with SA-β-gal staining. *n* = 5 for each group. Scale bars, 100 μm. (d) Western blot analysis of p21 and GAPDH in OA and 2 days after treatment with vehicle or 43 μM UBX0101. *n* = 2 for each group. (e) Western blot analysis of activated caspase-3 (cCasp-3) and actin in healthy chondrocytes (Non-SnCs) 1 or 2 days after treatment with vehicle or 43 μM UBX0101 from 2 independent experiments. All uncropped immunoblots in Supplementary Fig. 13.

Fig 4d and Supplementary 12d



Supplementary 12e



221  
222  
223

Supplementary Figure 13. Uncropped immunoblots from indicated figures.



224 **Supplementary Table 1. Primers sequences used for RT-PCR**

225

226

<b>Gene (Mice)</b>	<b>Forward primer (5'-3')</b>	<b>Reverse primer (5'-3')</b>
Cdkn2a	AATCTCCGCGAGGAAAGC	GTCTGCAGCGGACTCCATS
Cdkn1a	ATTCCATAGGCGTGGGACCT	TCCTGGGCATTTCCGGTCAC
Il6	GCTACCAAACCTGGATATAATCA GGA	CCAGGTAGCTATGGTACTCCAGA A
Mmp13	GGAGCCCTGATGTTTCCCAT	GTCTTCATCGCCTGGACCATA
Il1β	GTATGGGCTGGACTGTTTC	GCTGTCTGCTCATTACAG
Sox9	ACCCACAGCTCCCCTGAAG	CTCACCTTCAGTGGCAAGAGC
Col2a1	CCTCCGTCTACTGTCCACTGA	ATTGGAGCCCTGGATGAGCA
Acan	CGTTGCAGACCAGGAGCAAT	CGGTCATGAAAGTGGCGGTA
Runx2	GCCGGGAATGATGAGAATA	GGTGAAACTCTTGCCCTCGTC
Bglap	GGCGCTACCTTGGGTAAAGTG	GACCACTCCAGCACAACCTCC
Ctsk	GCACCCTTAGTCTTCCGCTC	ACCCACATCCTGCTGTTGAG
Rankl	GAGCACGAAAACTGGTCGG	AGGGTTGGACACCTGAATGC
Opg	CAGCCATTTGCACACCTCAC	TTAGAGATCTTGGCCAGCC
β-actin	CAACCGTGAAAAGATGACCC	GTAGATGGGCACAGTGTGGG

227

<b>Gene (human)</b>	<b>Forward primer (5'-3')</b>	<b>Reverse primer (5'-3')</b>
cdkn2a	AGCTGGAATTACACAGCTGC	GGACTGGCTTGCAATCTTGT
mmp3	CACTCACAGACCTGACTCGG	GAGTCAGGGGGAGGTCCATA
il6	CCCCTGACCCAACCACAAAT	ATTTGCCGAAGAGCCCTCAG
mmp13	TGGTCCAGGAGATGAAGACC	TCCTCGGAGACTGGTAATGG
il1β	GGACAAGCTGAGGAAGATGC	TCGTTATCCCATGTGTGCGAA
col2a1	CGCCGCTGTCCTTCGGTGTC	AGGGCTCCGGCTTCCACACAT
acan	TGGGAACCAGCCTATACCCCA G	CAGTTGCAGAAGGGCCTTCTGTA C
β-actin	GCTCCTCCTGAGCGCAAGTAC	GGACTCGTCATACTCCTGCTTGC